LEO-Satellite-Assisted UAV: Joint Trajectory and Data Collection for Internet of Remote Things in 6G Aerial Access Networks

Ziye Jia, Min Sheng, *Senior Member, IEEE*, Jiandong Li, *Senior Member, IEEE*, Dusit Niyato, *Fellow, IEEE*, and Zhu Han, *Fellow, IEEE*

***Abstract*—As the sixth generation (6G) network is under research, and one important issue is the aerial access network and terrestrial-space integration. The Internet of Remote Things (IoRT) sensors can access the unmanned aerial vehicles (UAVs) in the air, and low Earth orbit (LEO) satellite networks in the space help to provide lower transmission delay for delay-sensitive IoRT data. Therefore, in this article, we consider the LEO satellite-assisted UAV data collection for the IoRT sensors. Specifically, a UAV collects the data from the IoRT sensors, then two transmission modes for the collected data back to Earth: 1) the delay-tolerant data leveraging the carry-store mode of UAVs to Earth and 2) the delay-sensitive data utilizing the UAV-satellite network transmission to Earth. Considering the limited payloads of UAVs, we focus on minimizing the total energy cost (trajectory and transmission) of UAVs while satisfying the IoRT demands. Due to the intractability of direct solution, we deal with the problem using the Dantzig–Wolfe decomposition and design the column generation-based algorithms to efficiently solve the problem. Moreover, we present a heuristic algorithm for the subproblem to further reduce the complexity of large-scale networks. Finally, numerical results verify the efficiency of the proposed algorithms and the advantage of LEO satellite-assisted UAV trajectory design combined with the data transmission is also analyzed.**

***Index Terms*—6G, aerial access network, column generation, Dantzig–Wolfe, decomposition, Internet of Remote Things (IoRT), low Earth orbit (LEO) satellite, unmanned aerial vehicles (UAVs).**

I. Introduction

THE SIXTH generation (6G) system is attracting more and more attentions from both the industry and academia, and one important application in 6G is the aerial access network and terrestrial-space integration, which significantly benefits the Internet of Remote Things (IoRT) [1], [2]. Since environmental monitoring data in the remote areas, such as deserts, oceans, and many depopulated zones, provides important information of the world, but there are few base stations to collect the data in such areas. Fortunately, the aerial access network and terrestrial-space integration facilitate the IoRT data collection and transmission. Satellites in the space, unmanned aerial vehicles (UAVs) in the air, the ground station and data processing center, as well as the demands from Earth compose the aerial access and integrated terrestrial-space networks.

Satellites, including geostationary orbit (GEO), medium Earth orbit (MEO), and low Earth orbit (LEO), are the key components in the space to provide the global service [3]. Compared with GEO and MEO, LEO satellites are popular recently due to the lower development costs and since large-scale LEO satellite networks can guarantee lower transmission delay. For example, the 40 000 LEO satellite network is planned by SpaceX Starlink [4]. Although the satellite networks can guarantee the global coverage, it is still difficult for the IoRT sensors to directly connect with satellites due to the long distance between IoRT sensors and satellites, as well as the limited transmission power of small IoRT sensors [5]. Since the UAV flies in a low altitude and can provide flexible ubiquitous accessibility, it is taken into account to collect the data from the IoRT sensors [6], [7].

UAVs own the advantages of high-mobility and flexibility, which can provide ubiquitous coverage [8]. There are two types of UAV: 1) the rotary-wing UAV and 2) the fixed-wing UAV. Rotary-wing UAVs can realize vertical take-off and landing and can hover at a fixed point, but the mobility and power are very limited. Fixed-wing UAVs glide over the air with high speed and can be equipped with heavy payloads [9], [10]. Compared with the rotary-wing UAVs, fixed-wing UAVs have stronger payload ability, so we only consider the fixed-wing UAVs in this article. In the remaining of this article, UAVs refer to fixed-wing UAVs.

In this article, we consider the LEO satellite network-assisted UAV trajectory and transmission for the IoRT data collection. UAVs leverage the carry-store mode to bring the collected delay-tolerant data, e.g., the general environment

Manuscript received April 12, 2020; revised July 17, 2020 and August 20, 2020; accepted August 28, 2020. Date of publication September 2, 2020; date of current version June 7, 2021. This work was supported in part by the Natural Science Foundation of China under Grant U19B2025, Grant 61725103, Grant 61701363, and Grant 61931005; and in part by the Doctoral Students' Short-Term Study Abroad Scholarship Fund of Xidian University. *(Corresponding author: Min Sheng.)*

Ziye Jia, Min Sheng, and Jiandong Li are with the State Key Laboratory of ISN, Xidian University, Xi'an 710071, China (e-mail: ziyejia@stu.xidian.edu.cn; msheng@mail.xidian.edu.cn; jdli@mail.xidian.edu.cn).

Dusit Niyato is with the School of Computer Science and Engineering, Nanyang Technological University, Singapore 639798 (e-mail: dniyato@ntu.edu.sg).

Zhu Han is with the University of Houston, Houston, TX 77004 USA, and also with the Department of Computer Science and Engineering, Kyung Hee University, Seoul 446-701, South Korea (e-mail: zhan2@uh.edu).

Digital Object Identifier 10.1109/JIOT.2020.3021255

sensing data, back to the UAV ground station for further processing. In the carry-store mode, the delay is large and the data transmitted in this mode should be delay-tolerant. However, there also exists delay-sensitive data from the IoRT sensors, for example, the emergency information of disaster, which should be sent back to the ground data processing center within a limited time. Since LEO satellite networks are capable of transmitting data to Earth with low delay, the delay-sensitive data collected by UAVs can be relayed by LEO[1] satellite networks back to the ground data processing center. Since there are two types of IoRT data (delay-tolerant data and delay-sensitive data), we design a system combining two data transmission modes. As for the delay-tolerant IoRT data, the UAV carry-store mode is applied: the IoRT data are collected, stored, and carried by the UAV, flying with the UAV to the destination station and then using the high-speed optical cable transmitting to the data processing center. With regard to the delay-sensitive IoRT data, the UAV-based collection and satellite network relay mode is employed. In particular, the IoRT data collected by the UAV is transmitted to satellites, using the satellite-to-satellite (S2S) links [11] and satellite–ground station links transmitted to the ground station, then using the high-speed optical cable to the data processing center. Since the UAV energy capacity is very limited, and both propulsion and data transmission consume a large amount of energy, we focus on minimizing the total energy cost of UAVs while satisfying all the IoRT data demands and multiple constraints. The original problem is in the form of integer linear programming (ILP) which is NP-hard to solve. Especially, when the system is within a large scale, the brute-force searching has high complexity [12], [13]. Fortunately, constraints of original problem are characterized by a special structure, because if the complicating constraints are removed, the remaining constraints are in the form of a block angular structure, which can be further solved using the column generation [14] method. In addition, we utilize the Dantzig–Wolfe decomposition [15] to deal with the complicating constraints.

In particular, by combining the Dantzig–Wolfe decomposition and column generation as an efficient method to deal with the large-scale ILP problem, we reformulate the original problem into two coupled smaller problems: 1) a restricted master problem and 2) a set of pricing problems. The restricted master problem is initialized by a heuristic algorithm with a set of feasible solution. Then, the dual variable information from the linear programming relaxation of the restricted master problem is passed to the pricing problems to decide the new optimal objectives of different pricing problems. Since only a fraction of variables are considered in the restricted master problem, it can be efficiently solved. Moreover, since every pricing problem is independent with each other, all the pricing problems can be solved concurrently, which further accelerates the solution speed. These two problems are solved iteratively until the termination condition is satisfied. To further accelerate the solution, we design a heuristic algorithm for the pricing problems without affecting the final solution of restricted master problem.

For clarity, the main contributions of this work are listed as follows.

1) We propose a LEO satellite network-assisted UAV trajectory for the IoRT data collection. To the best of out knowledge, this is an innovative work considering the LEO satellite network for UAV data transmission. Furthermore, we present the model combined two transmission modes for the IoRT data back to Earth, including the UAV carry-store mode for the delay-tolerant data and the satellite network relay mode for the delay-sensitive data transmission. Considering the limited payloads of UAV and multiple energy consumption, a UAV energy cost minimization problem is formulated.
2) Due to the high-complexity of the problem, we propose a column generation-based algorithm to obtain the solution more efficiently. Moreover, to improve the solution complexity in a large-scale system, we present a heuristic algorithm to efficiently solve the pricing problems without affecting the optimal solution of the restricted master problem. The algorithm complexity is also analyzed.
3) Numerical results are provided, followed by the corresponding analyses which verify the efficiency of the proposed algorithms, and the advantage and insight of cooperation of two transmission modes for UAVs are also analyzed.

The remainder of this article is organized as follows. Literature reviews are provided in Section II. System model and the problem formulation are presented in Section III. In Section IV, the problem decomposition and algorithms are presented. Numerical results and corresponding analyses are provided in Section V. Finally, conclusions are drawn in Section VI.

II. Literature Review

There exists a couple of works related with the UAV-based service for the ground equipments. For example, Zhang *et al.* [16] designed a sense-and-send protocol by cellular-controlled UAVs, jointly considering the UAV trajectory, location, and scheduling optimization. Wang *et al.* [17] proposed a UAV-assisted Internet of Things (IoT) network, in which the UAV serves as an aerial data collector and an anchor node, assisting the base station for data collecting and device positioning. A framework jointly optimizing the placement and mobility of UAV is proposed in [18], which also consider the UAV-association and uplink power control. In [19], a cooperative UAV and base station mechanism for the IoT sensor data collection is proposed, including two transmission modes: 1) the collected data by UAV being directly transmitted to the cellular base station or 2) the collected data being transmitted to another UAV. These two transmission modes are jointly optimized. Chen *et al.* [20] presented a framework using UAV to serve the mobile users in the cloud radio access network, aiming at optimizing the quality of experience of wireless devices. Mozaffari *et al.* [21] analyzed the deployment of

[1]Since we only consider the LEO satellite, LEO satellite and satellite are interchangeably used in the rest of the paper.

UAVs as base stations for the device-to-device terrestrial user communication, and the tradeoff between delay and coverage are also discussed. Cheng *et al.* [22] developed a novel dynamic regular-shaped geometry-based channel model for the first time, which complements the existing channel models and becomes the cornerstone of cooperative communications. A UAV trajectory path planning mechanism is designed for the energy-efficient inspection in [23], considering multiple UAV energy consumption.

In regard to the cooperation of satellites and UAVs, Wang *et al.* [24] presented a resource allocation problem of UAVs in the single GEO satellite–UAV–ground network, jointly considering hovering and power control, aiming to reduce the multiple interference. Sharma and Kim [25] presented a decode-and-forward secure UAV-based relay for the satellite data transmitted to the ground. Li *et al.* [26] considered using the UAV to enhance the hybrid GEO satellite-maritime communication system. Specifically, UAV trajectory and power are optimized, considering the constraints of UAV kinematics, interference, backhaul, and energy capacity. A framework of UAV-based edge computing combined with satellite-based access to cloud computing is proposed in [27], and a learning-based algorithm is proposed for the computing offloading. Yan *et al.* [28] investigated the UAV- and satellite-based terrestrial user access in the emergency situations, and the competition of users as well as the choice for the UAV or satellite are also analyzed.

However, to the best of our knowledge, the cooperation of UAVs and LEO satellite networks have not been investigated in the existed works, as well as combining two transmission modes (UAV carry-store mode and satellite relay mode) has not been considered. Since the aerial access network and terrestrial-space integration are an important issue in 6G, the cooperation of UAVs and LEO satellite networks, and the corresponding challenges cannot be neglected.

III. System Model and Problem Formulation

First, in Section III-A, we introduce a scenario composed of LEO satellite networks in the space, UAVs in the air and IoRT sensors on the ground. Then, we present the LEO satellite-assisted UAV trajectory model for IoRT data collection in detail, including the UAV data collection in Section III-B, UAV data transmission in Section III-C, the UAV trajectory model in Section III-D, and the total energy cost model with budget limitation in Section III-E. The corresponding problem formulation is presented in Section III-F.

A. Scenario

We consider a LEO satellite network-assisted UAV trajectory and transmission for collecting IoRT data. As shown in Fig. 1, IoRT sensors $s_1 - s_5$ are scattered in a large region, where there exists no base stations and the data from these IoRT sensors are collected by UAVs. In Fig. 1, a UAV takes off from the departure station, flying and passing the IoRT sensors to collect data, and then land on the destination station. Two types of IoRT data are illustrated: the delay-tolerant IoRT data collected by the UAV is stored and carried by the UAV

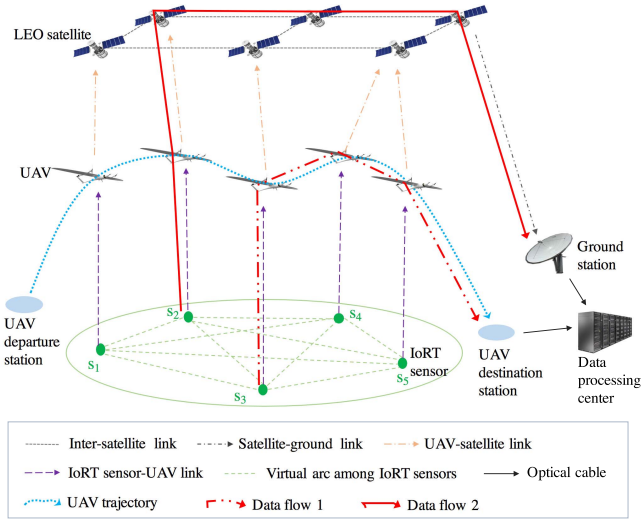

Fig. 1. Scenario of LEO satellite-aided UAV data collection and trajectory.

to the destination station, and then transmitted by the high-speed optical cable to the data processing center, depicted as data flow 1 from IoRT sensor s_3 in Fig. 1. With regard to the delay-sensitive IoRT data, since these data cannot tolerate the long delay of the UAV carry-store mode, the LEO satellite relay mode is employed: the UAV collected data is transmitted to a satellite and the data is sent back to the ground station with smaller delay using the S2S links and satellite–ground links, depicted by data flow 2 from IoRT sensor s_2 in Fig. 1. The data arrived at the ground station will be transmitted to the data processing center by the high-speed optical cable. The virtual bidirectional arcs among the IoRT sensors in Fig. 1 are deemed as the route choices for the UAV, because the shortest UAV trajectory between two IoRT sensors is the straight line between these two IoRT sensors.

We use $\mathcal{I}$ to denote the IoRT sensors, $i \in \mathcal{I}$. $\mathcal{U}$ indicates the set of UAVs, $u \in \mathcal{U}$. $\mathcal{S}$ represents the set of LEO satellites, $s \in \mathcal{S}$. $\mathcal{E}$ represents the virtual arcs among the IoRT sensors, $e(i, j) \in \mathcal{E}$, $i, j \in \mathcal{I}$ and $i \neq j$. ϕ_i is the data size of IoRT sensor $i \in \mathcal{I}$. D^u is the storage capacity of UAV $u \in \mathcal{U}$. E^u denotes the energy capacity of UAV $u \in \mathcal{U}$ and E_c^u denotes the total energy cost of UAV $u \in \mathcal{U}$. Key notations used in this article are listed in Table I.

B. UAV Data Collection

Since there are little blocking objects in the remote areas, the communication channels from the IoRT sensors to UAVs are line-of-sight, and the case with non-line-of-sight can be also considered easily. According to [29], the channel gain from the IoRT sensors to UAVs of the free-space model as

$$G_{iu} = \delta_0 / l_{iu}^2(t) \tag{1}$$

in which δ_0 indicates the reference channel gain at $l_{iu}(t) = 1$ m, and its value is related with the antenna gain, carrier frequency, and other factors. Hence, the channel capacity (in

TABLE I
KEY NOTATIONS

Symbol	Description
$\mathcal{I}$, $\mathcal{U}$, $\mathcal{S}$	The set of IoRT sensors, UAVs and satellites, $i \in \mathcal{I}$, $u \in \mathcal{U}$, $s \in \mathcal{S}$.
$\mathcal{E}$	Virtual arc set of among different IoRT nodes, $e(i,j) \in \mathcal{E}$, $i,j \in \mathcal{I}$, $i \neq j$.
ϕ_i	Data size of IoRT sensor $i \in \mathcal{I}$.
β_i	Parameter indicates whether the data of IoRT sensor $i \in \mathcal{I}$ is delay-tolerant. $\beta_i = 1$ if delay-tolerant, $\beta_i = 0$ if delay-sensitive.
D^u	Storage capacity of UAV $u \in \mathcal{U}$.
$P_{i^t}^{tr}$	Transmission power of IoRT sensor $i \in \mathcal{I}$ to UAV $u \in \mathcal{U}$ at time t.
B_{iu}^t	Bandwidth allocated to the channel from IoRT sensor $i \in \mathcal{I}$ to UAV $u \in \mathcal{U}$ at time t.
c_{iu}^t	Channel capacity from IoRT $i \in \mathcal{I}$ to UAV $u \in \mathcal{U}$ at time t.
$P_{u^t}^{tr}$	Transmission power of UAV $u \in \mathcal{U}$ to satellite $s \in \mathcal{S}$ at time t.
$P_{s^t}^{re}$	The received power of satellite $s \in \mathcal{S}$ from UAV $u \in \mathcal{U}$ at time t.
B_{us}^t	Bandwidth allocated to the channel from UAV $u \in \mathcal{U}$ to satellite $s \in \mathcal{S}$ at time t.
c_{us}^t	Channel capacity from UAV $u \in \mathcal{U}$ to satellite $s \in \mathcal{S}$ at time t.
v_u	Velocity of UAV $u \in \mathcal{U}$ in the intermediate phase.
T^u	The intermediate flight time cost of UAV $u \in \mathcal{U}$.
d_{ij}	The Euclidean distance between IoRT sensors i and j.
E^u	Energy capacity of UAV $u \in \mathcal{U}$,
E_c^u	Total energy cost of UAV $u \in \mathcal{U}$.
E_{ta}^u, E_f^u, E_{la}^u, E_{tran}^u	Energy cost for UAV $u \in \mathcal{U}$ taking off, intermediate flight, landing, and communication with satellites.
$x_{i^t}^u$	Binary variable $x_{i^t}^u \in \{0,1\}$ in P0 indicates whether UAV u flies through IoRT $i \in \mathcal{I}$.
$y_{i^t j^k}^u$	Binary variable $y_{i^t j^k}^u \in \{0,1\}$ in P0 indicates whether UAV u flies through virtual arc $e(i,j) \in \mathcal{E}$.
w_p^u	Binary variable $w_p^u \in \{0,1\}$ in P1 indicates whether UAV u flies as the trajectory path $p \in \mathcal{P}_u$.
$r_{i^t}^p$	Parameter in P1 indicates whether UAV trajectory $p \in \mathcal{P}_u$ flies through IoRT sensor $i \in \mathcal{I}$.
$u_{i^t j^k}^p$	Parameter in P1 denotes whether UAV trajectory $p \in \mathcal{P}_u$ passes through virtual arc $e(i,j) \in \mathcal{E}$.
x_{i^t}	Binary variable $x_{i^t}^u \in \{0,1\}$ in P4 indicates whether the trajectory of a certain UAV passes through IoRT sensor $i \in \mathcal{I}$.
$y_{i^t j^k}$	Binary variable $y_{i^t j^k}^u \in \{0,1\}$ in P4 indicates whether the trajectory of a certain UAV passes through virtual arc $e(i,j) \in \mathcal{E}$.

bit/s) from the IoRT sensors to UAVs can be calculated as

$$c_{iu}^t = B_{iu}^t \log_2\left(1 + \frac{P_{i^t}^{tr} G_{iu}}{\sigma^2}\right) = B_{iu}^t \log_2\left(1 + \frac{P_{i^t}^{tr} \gamma_0}{l_{iu}^2(t)}\right) \quad (2)$$

where B_{iu}^t denotes the bandwidth allocated to the channel from the IoRT sensor $i \in \mathcal{I}$ to UAV $u \in \mathcal{U}$ at time t, $P_{i^t}^{tr}$ is the transmission power of IoRT sensor $i \in \mathcal{I}$ at time t, σ^2 indicates the noise power, and $\gamma_0 = \delta_0/\sigma^2$ denotes the reference signal-to-noise ratio (SNR) [30].

Since the sparse distribution of the IoRT sensors and each IoRT sensor can only connect with one UAV, the interference is negligible. In addition, following [31], even there are additional interferences at the receiver, we suppose the aggregate interference in a Gaussian distribution and the corresponding power is incorporated into the noise term σ^2.

C. UAV Data Transmission

1) UAV-Satellite Mode: Since UAVs fly at the clear altitude and the connection between UAVs and satellites obtains light-of-sight. The communication channels between UAVs and satellites are mostly related with the UAV-to-satellite (U2S) distance. According to [32], the received power of satellite $s \in \mathcal{S}$ from UAV $u \in \mathcal{U}$ at time t is represented as

$$P_{s^t}^{re} = \frac{P_{u^t}^{tr} G_u^{tr} G_s^{re} c}{4\pi f l_{us}^t} \quad (3)$$

in which $P_{u^t}^{tr}$ is the transmission power from UAV $u \in \mathcal{U}$ to satellite $s \in \mathcal{S}$ at time t. G_u^{tr} and G_s^{re} are the transmission antenna gain of the UAV and the receiver antenna gain of the satellite, respectively. c is the speed of light. f is the carrier frequency and l_{us}^t is the distance between UAV $u \in \mathcal{U}$ and satellite $s \in \mathcal{S}$ at time t. Therefore, the channel capacity (in bit/s) from UAVs to satellites is calculated as

$$\begin{aligned} c_{us}^t &= B_{us}^t \log_2\left(1 + \frac{P_{s^t}^{re}}{k_B T_s B_{us}^t}\right) \\ &= B_{us}^t \log_2\left(1 + \frac{P_{u^t}^{tr} G_u^{tr} G_s^{re} c}{4\pi f l_{us}^t k_B T_s B_{us}^t}\right) \end{aligned} \quad (4)$$

where B_{us}^t represents the bandwidth between UAV $u \in \mathcal{U}$ and satellite $s \in \mathcal{S}$ at time t, k_B is the Boltzmann's constant, and T_s indicates the system noise temperature. In particular, the practical system always guarantees $c_{us}^t \gg c_{iu}^t$. Hence, this constraint is not further discussed in the rest of this article.

The total energy cost of UAV $u \in \mathcal{U}$ to transmit the collected time-sensitive data ϕ_i to satellite $s \in \mathcal{S}$ is calculated as

$$E_{tran}^u = \sum_{i \in \mathcal{I}} \frac{x_{i^t}^u P_{u^t}^{tr} (1 - \beta_i) \phi_i}{c_{us}^t} \quad (5)$$

in which the binary variable $x_{i^t}^u \in \{0,1\}$ indicate whether the data from IoRT $i \in \mathcal{I}$ is collected by UAV $u \in \mathcal{U}$ at time t

$$x_{i^t}^u = \begin{cases} 1, & \text{data from IoRT } i \in \mathcal{I} \text{ is collected by UAV } u \in \mathcal{U} \\ 0, & \text{otherwise.} \end{cases} \quad (6)$$

Parameter β_i indicates whether the data of IoRT sensor $i \in \mathcal{I}$ is delay-tolerant. $\beta_i = 1$ if delay-tolerant, and $\beta_i = 0$ if delay-sensitive. The delay-sensitive data collected by UAV $u \in \mathcal{U}$ at time t will be transmitted by the nearest satellite $s \in \mathcal{S}$ and the data transmission consumes UAV's energy. Since the speed of satellites is much larger than the speed of UAVs, we only consider the connection switching between UAVs and satellites due to the periodical movement of satellites. Besides, due to the large coverage of satellites, the connection duration between a UAV and a LEO satellite can last several minutes at least [27] and, therefore, the connection between the UAV and LEO satellite is not changing instantaneously. The delay-sensitive data should be relayed by the satellite network, and the link capacity between UAVs and satellites is larger than the link capacity between IoRT sensors and UAVs, and thus the data collection and transmission can be conducted by UAVs concurrently [33].

2) UAV Carry-Store Mode: For the delay-tolerant IoRT data, the UAV carry-store mode is used due to the low cost of storage payload. Specifically, the collected delay-tolerant IoRT data will be stored and carried by the UAV to the destination station for further processing, shown as data flow 2 in Fig. 1. Note that during the flight of the UAV, the total collected delay-tolerant data size stored in the UAV should not exceed the UAV storage capacity D^u

$$\sum_{i\in\mathcal{I}} \phi_i x_{i^t}^u \beta_i \le D^u \quad \forall u \in \mathcal{U}. \tag{7}$$

D. UAV Trajectory

The energy cost of UAV trajectory mostly consists three parts: 1) acceleration (taking off); 2) constant speed intermediate phase; and 3) deceleration phase (landing) [34]. According to [31], after taking off and before landing on, the UAV is assumed to fly at a fixed altitude. We define that the UAV energy cost of taking off and landing on are E_{ta}^u and E_{la}^u, respectively. Additionally, following [31] and [33], in the intermediate phase, the propulsion energy of the UAV in the flight period is expressed as

$$E_f^u = \int_0^{T^u} \left[\kappa_1 \cdot \|v_u(t)\|^3 + \frac{\kappa_2}{\|v_u(t)\|} \cdot \left(1 + \frac{\|a_u(t)\|^2}{g^2}\right)\right] dt \tag{8}$$

in which κ_1 and κ_2 are fixed parameters related with the air density, UAV's weight, wing area, etc. $v_u(t)$ and $a_u(t)$ are the velocity and acceleration of UAV $u \in \mathcal{U}$ at time t, respectively. g is the gravitational acceleration (a constant of 9.8 m/s^2). Therefore, the energy consumption of UAV trajectory depends on its velocity and acceleration. Since the speed of UAV in the intermediate segment is thought as a constant in our problem, i.e., $a_u(t) = 0$ and $v_u(t)$ is a constant v_u, we have

$$E_f^u = T^u \cdot \left(\kappa_1 {v_u}^3 + \frac{\kappa_2}{v_u}\right). \tag{9}$$

The intermediate flight time of UAV u is calculated as

$$T^u = \frac{\sum_{e(i,j)\in\mathcal{E}} y_{i^t j^k}^u d_{ij}}{v_u} \tag{10}$$

where binary variable $y_{i^t j^k}^u \in \{0, 1\}$ indicates whether UAV $u \in \mathcal{U}$ flies through virtual arc $e(i, j)$, and $y_{i^t j^k}^u = 1$ means that UAV u visits IoRT sensor j at time k after visiting IoRT sensor i at time t, $t \le k$

$$y_{i^t j^k}^u = \begin{cases} 1, & \text{if UAV } u \in \mathcal{U} \text{ flies through virtual arc } e(i,j) \\ 0, & \text{otherwise.} \end{cases} \tag{11}$$

d_{ij} denotes the Euclidean distance between IoRT sensors $i \in \mathcal{I}$ and $j \in \mathcal{I}$.

E. Energy Cost Model

The energy cost of the fixed-wing UAV in this model mainly includes the following parts: propulsion cost for trajectory, the constant cost for taking off and landing, and the data transmission cost with satellites.

In detail, the total energy cost of the UAV trajectory is

$$E_{traj}^u = E_{ta}^u + E_{la}^u + E_f^u. \tag{12}$$

The total energy cost of the UAV is composed of trajectory and communication with satellites, i.e.,

$$E_c^u = E_{traj}^u + E_{\text{tran}}^u = E_{ta}^u + E_{la}^u + E_f^u + E_{\text{tran}}^u. \tag{13}$$

Since E_{ta}^u and E_{la}^u are constant, we omit these two terms for brevity in the following optimization problems, i.e., $E_c^u = E_f^u + E_{\text{tran}}^u$.

F. Problem Formulation

Since the UAV energy budget is limited, and both trajectory and data transmission consume a large amount of energy, we consider to minimize the total energy consumption while all the IoRT data are satisfied. This problem is formulated as P0

$$\text{(P0)}: \min_{\boldsymbol{x},\boldsymbol{y}} \sum_{u\in\mathcal{U}} E_c^u \tag{14}$$

$$\text{s.t.} \sum_{u\in\mathcal{U}} x_{i^t}^u = 1 \quad \forall i \in \mathcal{I} \tag{15}$$

$$\sum_{j\in\mathcal{I}} y_{o^t j^k}^u = 1 \quad \forall u \in \mathcal{U} \tag{16}$$

$$\sum_{i\in\mathcal{I}} y_{i^t d^k}^u = 1 \quad \forall u \in \mathcal{U} \tag{17}$$

$$\sum_{e(i,j)\in\mathcal{E}} y_{i^t j^k}^u = \sum_{e(j,i)\in\mathcal{E}} y_{j^k i^t}^u \quad \forall u \in \mathcal{U}, \quad j \in \mathcal{I} \tag{18}$$

$$\sum_{i\in\mathcal{I}} \phi_i x_{i^t}^u \beta_i \le D^u \quad \forall u \in \mathcal{U} \tag{19}$$

$$E_c^u \le \theta \cdot E^u \quad \forall u \in \mathcal{U} \tag{20}$$

$$x_{j^k}^u \le \sum_{e(i,j)\in\mathcal{E}} y_{i^t j^k}^u \quad \forall u \in \mathcal{U}, \quad j \in \mathcal{I} \tag{21}$$

$$x_{i^t}^u \in \{0, 1\} \quad \forall u \in \mathcal{U}, i^t \in \mathcal{I} \tag{22}$$

$$y_{i^t j^k}^u \in \{0, 1\} \quad \forall u \in \mathcal{U}, \quad e(i, j) \in \mathcal{E} \tag{23}$$

where $\boldsymbol{x} = \{x_{i^t}^u \ \forall u \in \mathcal{U}, i \in \mathcal{I}\}$ and $\boldsymbol{y} = \{y_{i^t j^k}^u \ \forall u \in \mathcal{U}, e(i, j) \in \mathcal{E}\}$. Equation (15) denotes that each IoRT sensor $i \in \mathcal{I}$ can only be connected with one UAV u. Equations (16)–(18) are flow constraints. Equations (16) and (17) refer to the UAV trajectory

starts from departure origin and ends at the destination, respectively. Equation (18) indicates that a flow conservation should satisfied for a middle node in the UAV trajectory. Equation (19) indicates that the total delay-tolerant data size cannot exceed the storage capacity of UAV u. Equation (20) denotes that the total energy cost cannot exceed the energy capacity of UAV u, and θ is the empirical power efficiency. Equation (21) is the coupled constraint between $\boldsymbol{x}$ and $\boldsymbol{y}$.

IV. Algorithm Design

First, we analyze and decompose problem P0 according to the Dantzig–Wolfe decomposition in Section IV-A. The column generation-based algorithms are designed for the decomposed problems in Section IV-B. Finally, algorithm complexity is analyzed in Section IV-C.

A. Problem Decomposition

Note that problem P0 is in the form of ILP which is NP-hard to solve [12], let alone obtaining optimal solutions. According to [35], the time complexity of brute-force searching for problem P0 is $\mathcal{O}(N_1 \cdot N_2 \cdot 2^{N_1})$, in which N_1 is the number of variables and N_2 is the number of constraints. Specifically, in P0, $N_1 = N_{\boldsymbol{x}} + N_{\boldsymbol{y}} = |\mathcal{U}| \cdot |\mathcal{I}| + (1/2)(|\mathcal{U}| \cdot |\mathcal{I}|^2 + |\mathcal{U}| \cdot |\mathcal{I}|)$ and $N_2 = |\mathcal{I}| + 4 \cdot |\mathcal{U}| + 2 \cdot |\mathcal{U}| \cdot |\mathcal{I}|$. Hence, the time complexity of brute-force searching for P0 is $\mathcal{O}((2 \cdot |\mathcal{U}|^2 \cdot |\mathcal{I}|^3 + |\mathcal{U}| \cdot |\mathcal{I}|^3 + 6 \cdot |\mathcal{U}|^2 \cdot |\mathcal{I}|^2 + |\mathcal{U}| \cdot |\mathcal{I}|^2 + 4 \cdot |\mathcal{U}|^2 \cdot |\mathcal{I}|) \cdot 2^{(1/2)(|\mathcal{U}| \cdot |\mathcal{I}|^2 + |\mathcal{U}| \cdot |\mathcal{I}|)})$, according with the exponential complexity and the curse of dimensionality.

If constraint (15) of P0 is removed, the remaining constraints of P0 are in the structure of block triangular, which facilitates problem P0 to be decomposed into two smaller problems and solved by the column generation method [36]. Such a decomposition is based on the Dantzig–Wolfe decomposition. In particular, the Dantzig–Wolfe decomposition is designed for solving the large-scale ILP with block triangular structure [37], relying on the column generation to improve the tractability of the original problem. P0 can be equivalently reformulated into P1 (master problem), and then P3 (linear programming relaxation of restricted master problem) is solved by a small set of active columns, and P4 (pricing problems) are concurrently solved utilizing the triangular structure to dynamically generate the new columns for P3 to improve the objective. The problems P1, P2, P3, and P4 will be presented in detail later. Such iterations between the restricted master problem and pricing problems are terminated until the objective of the restricted master problem cannot be improved by any new columns from the pricing problems. The overview of the column generation method is depicted in Fig. 2. In addition, the original problem P0 and master problem P1 are equivalent, and the proof is in Proposition 1.

Proposition 1: Problem P0 (original problem) can be equivalently transformed to problem P1 (master problem)

$$\text{(P1)}: \min_{\boldsymbol{w}} \sum_{u \in \mathcal{U}} E_c^u \tag{24}$$

$$\text{s.t.} \sum_{p \in \mathcal{P}_u} w_p^u = 1 \quad \forall u \in \mathcal{U} \tag{25}$$

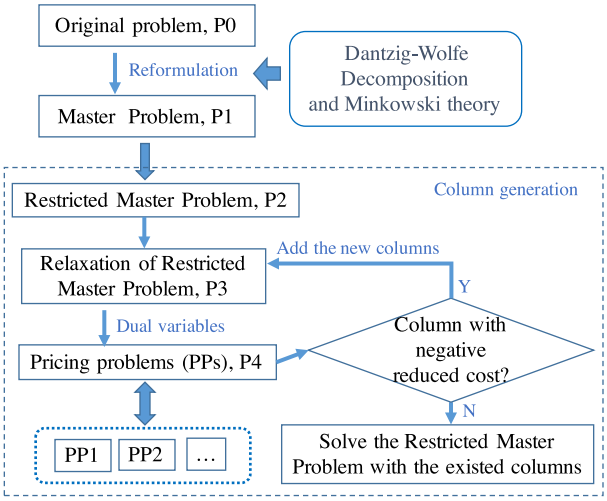

Fig. 2. Column generation overview.

$$\sum_{u \in \mathcal{U}} \sum_{p \in \mathcal{P}_u} w_p^u r_{i^t}^p = 1 \quad \forall i \in \mathcal{I} \tag{26}$$

$$w_p^u \in \{0, 1\} \quad \forall p \in \mathcal{P}_u, \quad u \in \mathcal{U} \tag{27}$$

where $\boldsymbol{w} = \{w_p^u \quad \forall p \in \mathcal{P}_u, u \in \mathcal{U}\}$.

Proof: According to the Minkowski's theory [14], i.e., an interior point of the convex hull can be expressed as the linear combination of the extreme points of the convex hull. In detail, we have

$$\left\{ x_{i^t}^u = \sum_{p \in \mathcal{P}_u} w_p^u r_{i^t}^p \mid \sum_{p \in \mathcal{P}_u} w_p^u = 1, w_p^u \in \{0, 1\} \right\} \tag{28}$$

and

$$\left\{ y_{i^t j^k}^u = \sum_{p \in \mathcal{P}_u} w_p^u u_{i^t j^k}^p \mid \sum_{p \in \mathcal{P}_u} w_p^u = 1, w_p^u \in \{0, 1\} \right\} \tag{29}$$

in which both $r_{i^t}^p \in \{0, 1\}$ and $u_{i^t}^p \in \{0, 1\}$ represent the extreme points of the convex hull $\mathcal{P}$. The convex hull $\mathcal{P}$ is formed by the polytope of constraints (16)–(21) and $\mathcal{P} = \{\mathcal{P}_u, u \in \mathcal{U}\}$, i.e., $\mathcal{P}$ is composed of smaller convex hull $\mathcal{P}_u$ corresponding to each UAV $u \in \mathcal{U}$. Hence, the variables $x_{i^t}^u$ and $y_{i^t j^k}^u$ in P0 can be represented into (28) and (29), respectively. Extreme points $r_{i^t}^p \in \{0, 1\}$ indicates whether UAV trajectory path $p \in \mathcal{P}_u$ passes through IoRT $i \in \mathcal{I}$, and $u_{i^t j^k}^p \in \{0, 1\}$ denotes whether UAV trajectory path $p \in \mathcal{P}_u$ passes through $e(i, j) \in \mathcal{E}$. $w_p^u \in \{0, 1\}$ represents the coefficients of the extreme points [15]. By substituting the redefinitions (28) and (29) into P0, we can obtain P1. Binary variable $w_p^u \in \{0, 1\}$ in P1 indicates whether UAV $u \in \mathcal{U}$ flies as the trajectory path $p \in \mathcal{P}_u$ due to that there are a great number of paths to choose for a UAV trajectory. $r_{i^t}^p \in \{0, 1\}$ and $u_{i^t j^k}^p \in \{0, 1\}$ are the corresponding parameters in P1. Therefore, it is an equivalent transformation from P0 to P1. ■

As a result, E_c^u is updated as

$$E_c^u = E_f^u + E_{\text{tran}}^u$$

$$= \frac{\sum_{e(i,j)\in\mathcal{E}}\sum_{p\in\mathcal{P}_u} w_p^u u_{i^t j^k}^p d_{ij}}{v_u}\left(\kappa_1 {v_u}^3 + \frac{\kappa_2}{v_u}\right) + \frac{\sum_{i\in\mathcal{I}}\sum_{p\in\mathcal{P}_u} w_p^u r_{i^t}^p P_{u^t}^{tr}(1-\beta_i)\phi_i}{c_{us}^t}. \quad (30)$$

Moreover, such a reformulation can provide tighter solution for P0, and P1 can be solved in a smaller trajectory path solution set and complexity is reduced.

It is observed that P1 is still an ILP problem and NP-hard to solve because the number of possible trajectory paths is huge. However, we can utilize the column generation to deal with P1 with tractability. P1 only needs to be solved from a small trajectory path set (each UAV $u \in \mathcal{U}$ is initialized with one feasible trajectory path) and the new trajectory paths will be added to P1 in each iteration from the pricing problems. Since in each iteration, the solution set $\mathcal{P}_u' \subseteq \mathcal{P}_u$ for the master problem P1 is partially selected and enlarged, we define the restricted master problem as P2

$$\text{(P2)}: \min_{\boldsymbol{w}} \sum_{u\in\mathcal{U}} E_c^u \quad (31)$$

$$\text{s.t.} \sum_{p\in\mathcal{P}_u'} w_p^u = 1 \quad \forall u \in \mathcal{U} \quad (32)$$

$$\sum_{u\in\mathcal{U}}\sum_{p\in\mathcal{P}_u'} w_p^u r_{i^t}^p = 1 \quad \forall i \in \mathcal{I} \quad (33)$$

$$w_p^u \in \{0,1\} \quad \forall p \in \mathcal{P}_u', \quad u \in \mathcal{U}. \quad (34)$$

P2 is initialized by a feasible solution set $\mathcal{P}_u'$ and each UAV u has a feasible trajectory path in the initial set. Then, the linear programming relaxation of P2, i.e., P3 is solved to obtain the dual variables μ_u and μ_i, respectively, corresponding to constraints (32) and (33), $\boldsymbol{\mu} = \{\mu_u, \mu_i\}$

$$\text{(P3)}: \min_{\boldsymbol{w}} \sum_{u\in\mathcal{U}} E_c^u \quad (35)$$

$$\text{s.t. (32), (33)}$$

$$w_p^u \in [0,1] \quad \forall p \in \mathcal{P}_u', \quad u \in \mathcal{U}. \quad (36)$$

Then, $\boldsymbol{\mu}$ is provided to pricing problem P4. Specifically, using the existed columns, the Lagrange function of P3 is calculated in (37), shown at the bottom of the page. Then, we can obtain the objective η of the pricing problem:

$$\eta = \left(\kappa_1 {v_u}^2 + \frac{\kappa_2}{{v_u}^2}\right)\sum_{e(i,j)\in\mathcal{E}} d_{ij} y_{i^t j^k} + \sum_{i\in\mathcal{I}}\left(\frac{1}{c_{us}^t} P_u^{tr}(1-\beta_i)\phi_i - \mu_i\right) x_{i^t} - \mu_u \quad (38)$$

where $x_{i^t} \in \{0,1\}$ indicates whether the trajectory of a certain UAV passes through IoRT $i \in \mathcal{I}$ and $y_{i^t j^k} \in \{0,1\}$ indicates whether the trajectory of a certain UAV passes through virtual arc $e(i,j) \in \mathcal{E}$. The pricing problem is shown in P4

$$\text{(P4)}: \min_{\boldsymbol{x'},\boldsymbol{y'}} \ \eta \quad (39)$$

$$\text{s.t.} \sum_{j\in\mathcal{I}} y_{o^t j^k} = 1 \quad (40)$$

$$\sum_{i\in\mathcal{I}} y_{i^t d^k} = 1 \quad (41)$$

$$\sum_{e(i,j)\in\mathcal{E}} y_{i^t j^k} = \sum_{e(j,i)\in\mathcal{E}} y_{j^k i^t} \quad \forall, j \in \mathcal{I} \quad (42)$$

$$\sum_{i\in\mathcal{I}} \phi_i x_{i^t} \beta_i \le D^u \quad (43)$$

$$E_c^u \le \theta \cdot E^u \quad (44)$$

$$x_{j^k} \le \sum_{e(i,j)\in\mathcal{E}} y_{i^t j^k} \quad \forall j \in \mathcal{I} \quad (45)$$

$$x_{i^t} \in \{0,1\} \quad \forall i \in \mathcal{I} \quad (46)$$

$$y_{i^t j^k} \in \{0,1\} \quad \forall e(i,j) \in \mathcal{E} \quad (47)$$

in which $\boldsymbol{x'} = \{x_{i^t} \in \{0,1\}\ \forall i \in \mathcal{I}\}$ and $\boldsymbol{y'} = \{y_{i^t j^k} \in \{0,1\}\ \forall e(i,j) \in \mathcal{E}\}$. Constraints (40)–(45) in P4 have the same physical meaning with constraints (16)–(21) in P0, respectively. P4 is designed to find a feasible trajectory path with the highest reduced cost. The objective η of P4 is the reduced cost which is also used to decide the termination condition of the iterations between P3 and P4. If $\eta < 0$, the new generated columns from solving P4 are added to P3. Otherwise, if $\eta \ge 0$, the new generated columns from solving P3 are not further added to P3 and P3 is solved based on the existed columns to obtain the optimal solution. Moreover, due to the triangular block structure, each UAV $u \in \mathcal{U}$ has a corresponding pricing problem P4 and these pricing problems are independent with each other and can be solved concurrently, which further accelerate the iteration between P3 and P4.

B. Algorithm Design

The detailed column generation-based algorithm is shown in Algorithm 1. First, the restricted master problem should be initialized with a set of feasible solutions using Algorithm 2. In other words, each UAV is initialized with a feasible trajectory path and the dual variables $\boldsymbol{\mu}$ of P3 are obtained and given to pricing problems P4 to update the objective. Then, all P4 of different UAVs are solved concurrently using the optimization tool GUROBI, and the solutions of P4 are the new columns with favorable reduced cost for P3. Note that the reduced cost η is used to decide whether the new generated columns are further added to P3. If $\eta < 0$, the new generated columns are added to P3. Otherwise if $\eta \ge 0$, the new generated columns are not added to P3, and P3 is solved using the

$$\mathcal{L}(\boldsymbol{w},\boldsymbol{\mu}) = \sum_{e(i,j)\in\mathcal{E}}\sum_{p\in\mathcal{P}_u'}\left(\kappa_1 {v_u}^2 + \frac{\kappa_2}{{v_u}^2}\right) u_{i^t j^k}^p d_{ij} w_p^u + \frac{1}{c_{us}^t}\sum_{i\in\mathcal{I}}\sum_{p\in\mathcal{P}_u'} r_{i^t}^p P_u^{tr}(1-\beta_i)\phi_i w_p^u + \sum_{u\in\mathcal{U}}\mu_u + \sum_{i\in\mathcal{I}}\mu_i - \sum_{u\in\mathcal{U}}\sum_{p\in\mathcal{P}_u'}\mu_u w_p^u - \sum_{i\in\mathcal{I}}\sum_{u\in\mathcal{U}}\sum_{p\in\mathcal{P}_u'}\mu_i r_{i^t}^p w_p^u \quad (37)$$

Algorithm 1 Column Generation Algorithm

Input: Virtual IoRT network topology $(\mathcal{I}, \mathcal{E})$, IoRT data information ϕ_i, β_i, IoRT sensor transmission power P_{it}^{tr}, number of UAV $|\mathcal{U}|$, UAV storage capacity D^u, and UAV transmission power P_{ut}^{tr}.

Output: $\boldsymbol{x}$, $\boldsymbol{y}$, and the objective value of P0.

1: Initialize P2 with a set of feasible solutions by Algorithm 2.
2: Solve P3 and obtain dual variables $\boldsymbol{\mu}$ and update the objective for P4.
3: Solve P4 of each UAV to obtain the new columns and the reduced cost η.
4: **if** $\eta < 0$ **then**
5: Add the new generated columns to P3, and go to line 2.
6: **else**
7: Solve P3 using the existed columns to obtain the optimal solution.
8: **if** the solution of P3 is not integer **then**
9: Using approximation Algorithm 4 to obtain the integer solution.
10: **end if**
11: **end if**

Algorithm 2 Initialization for Problem P2

1: **for** $u \leq |\mathcal{U}|$ **do**
2: **if** $\mathcal{I} \neq \emptyset$ **then**
3: Using the resource constrained shortest path method to find the elementary trajectory path within $(\mathcal{I}, \mathcal{E})$ for UAV u.
4: Delete the corresponding IoRT nodes and virtual arcs in the trajectory of UAV u, i.e., $\mathcal{I} = \mathcal{I} \backslash \mathcal{I}_u$ and $\mathcal{E} = \mathcal{E} \backslash \mathcal{E}_u$.
5: **end if**
6: **end for**

Algorithm 3 Algorithm for Problem P4

1: Using the Yen's algorithm to generate K shortest trajectory paths (column set) for UAV u.
2: **for** $k \leq K$ **do**
3: Randomly choose one trajectory path from the set and compute the total energy cost E_c^u of the path.
4: **if** $E_c^u \leq E^u$ **then**
5: go to line 10.
6: **else**
7: Delete the current trajectory path from the set and go to line 3.
8: **end if**
9: **end for**
10: Compute the corresponding reduced cost η.
11: **if** $\eta < 0$ **then**
12: Return the new generated column.
13: **else**
14: Solve each pricing problem using branch and bound method to obtain the new column and update the reduced cost η.
15: **if** $\eta \geq 0$ **then**
16: Return $\emptyset$.
17: **end if**
18: Return the new generated column.
19: **end if**

existed columns. If the final solutions of P3 are integer, these integer solutions are also the optimal solutions for P2, P1 and P0 [38]. If the final solutions of P3 are fractional, we will further employ the approximation method in Algorithm 4 to acquire suboptimal solutions for P2.

Algorithm 2 is designed to obtain the feasible initialized solution for the restricted master problem P2 (as well as P3). Sequentially obtaining an elementary trajectory path for each UAV using the resource constrained shortest path-based method [39]. Specifically, in the restricted master problem, first, the shortest path is generated, and if no resource (energy, storage) constraint is violated, the path is deemed as an elementary path. Otherwise, the second shortest path is generated and the resource constraints are identified. Such a process is executed until a feasible elementary path is generated. Note that after the elementary trajectory path of each UAV is found, IoRT nodes as well as virtual arcs are updated by deleting the satisfied nodes and corresponding arcs, i.e., $\mathcal{I} = \mathcal{I} \backslash \mathcal{I}_u$ and $\mathcal{E} = \mathcal{E} \backslash \mathcal{E}_u$, in which $\mathcal{I}_u$ and $\mathcal{E}_u$ are the nodes and virtual arcs in the trajectory path of UAV u.

To speed up the solution of P4, Algorithm 3 is designed, based on the fact that it is not necessary to find the optimal solution of P4 in each iteration between P3 and P4. We consider using the heuristic method for P3 to obtain the favorable columns because obtaining the optimal solution is time consuming. In detail, we employ the Yen's algorithm [40] to generate the K shortest trajectory paths for each UAV and randomly select one path from the set as the new column. Then, the corresponding reduced cost η is computed and if $\eta < 0$, the column is found and added to P3. Note that $\eta \geq 0$ does not mean that there is no column exists, so if columns with favorable reduced cost cannot be found using the heuristic method, the branch and bound method is applied to obtain the optimal solution and update η of P4. If the updated solution with $\eta \geq 0$, there is no favorable column exist, and if $\eta < 0$, the new columns are generated. The reason to produce K feasible trajectory paths in line 1 of Algorithm 3 is that different UAVs depart from the same depot and land on the same destination station, each UAV has the same shortest trajectory path. K feasible trajectory paths can guarantee the diversity of the new generated columns.

When the column generation iteration terminates, P3 is solved to optimal using the current columns. If the last solution of P3 is integer, that is to say, the optimal solution of P1 is also found, i.e., the lower bound of the designed Algorithm 1. However, if the last solution of P3 is fractional, we cannot simply round off the fractional variables because such solutions are not favorable and even not feasible [41]. Therefore, we design Algorithm 4 to finally obtain the approximated integer solution for P2. As for each UAV u, selecting the trajectory

Algorithm 4 Approximation Integer Solution for Problem P2

1: **for** $u \leq |\mathcal{U}|$ **do**
2: Select the trajectory path with the largest w_p^u from $\mathcal{P}_u'$.
3: **if** the number of such trajectory paths is more than one **then**
4: Select the trajectory with the least E_c^u.
5: **end if**
6: Round off the corresponding w_p^u to 1.
7: **if** the rounded trajectory path is not feasible **then**
8: Delete this rounded trajectory path from $\mathcal{P}_u'$ and go to 2.
9: **end if**
10: **end for**
11: **Return** the integral trajectory path set.

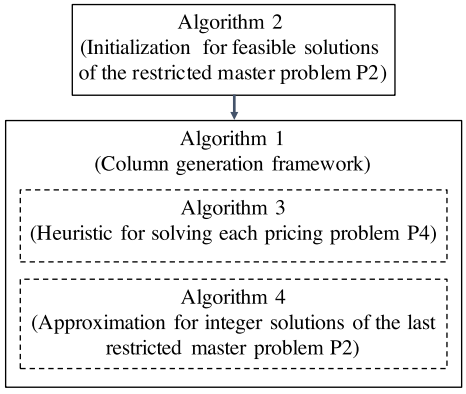

Fig. 3. Relations among the proposed algorithms.

path with the largest w_p^u from $\mathcal{P}_u'$ and rounding off the corresponding w_p^u to 1, because such a trajectory path is more likely to be the optimal choice. Then, the feasibility of the integral trajectory path is checked because the resource constraints may be violated. If the integral trajectory path is not feasible, it is deleted from the set $\mathcal{P}_u'$ and another fractional trajectory path is selected and further processed.

The relations among the proposed algorithms are depicted in Fig. 3. Algorithm 2 is used to obtain the feasible initial solutions for the restricted master problem P2 and Algorithm 1 provides the total column generation framework, in which Algorithm 3 is an efficient heuristic method to solve the pricing problem P4. Finally, when the iteration between P3 and P4 terminates, Algorithm 4 is employed to obtain the approximated integer solutions for the restricted master problem P2, i.e., the final solutions for P1 and P0.

C. Complexity Analysis

Since in the column generation algorithm, the tractable part is the solution for ILP problem P4. Similar to the complexity discussed at the beginning of Section IV-A, the time complexity of brute-force searching for P4 is $\mathcal{O}(N_1' \cdot N_2' \cdot 2^{N_1'})$, in which $N_1' = (1/2)(|\mathcal{I}|^2 + |\mathcal{I}|)$ is the number of variables and $N_2' = 2 \cdot |\mathcal{I}| + 4$ is the number of constraints of P4. Hence, the complexity of brute-force searching for P4 is $\mathcal{O}((|\mathcal{I}|^3 + 5 \cdot |\mathcal{I}|^2 + 6 \cdot |\mathcal{I}|) \cdot 2^{(1/2)(|\mathcal{I}|^2 + |\mathcal{I}|)})$. Although it is still with the exponential complexity, both the coefficient and exponent are reduced compared with directly solving P0. Moreover, Algorithm 3 is also designed for P4 and it further reduced the time complexity.

TABLE II
SIMULATION PARAMETERS

Parameter	Value	Parameter	Value
ϕ_i	[10,100]Mbits	v_u	50m/s
D^u	10Gbits	E^u	100KJ
γ_0	80dB	θ	70%
P_{it}^{tr}	0.5W	B_{us}^t	54MHz
B_{iu}^t	2MHz	f	2.4GHz
P_{ut}^{tr}	10W	$G_u^{tr} G_s^{re}$	15dB
κ_1	9.26×10^{-4}kg/m	κ_2	2,250kg $\cdot$ m^3/s^4
UAV altitude	1km	Satellite altitude	780km

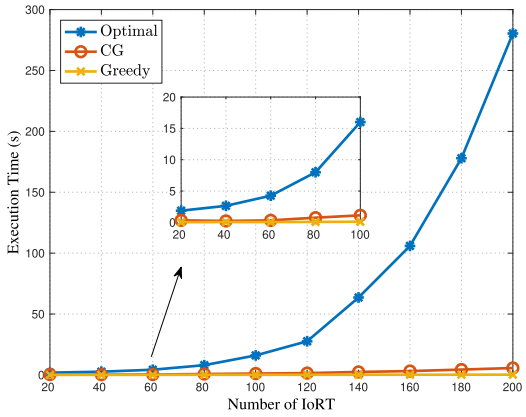

(a)

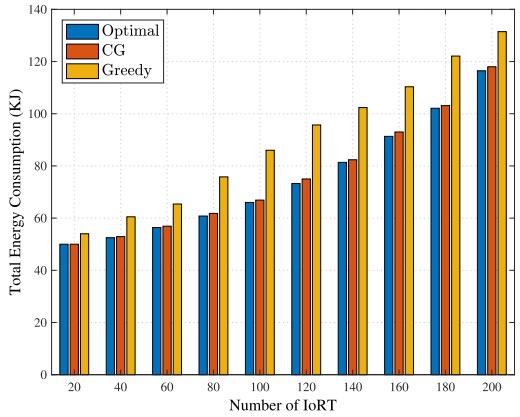

(b)

Fig. 4. Time complexity and energy cost results from different algorithms with $|\mathcal{U}| = 2$. (a) Time consumption *versus* number of IoRT. (b) Total energy cost *versus* number of IoRT.

V. NUMERICAL RESULTS

We conduct a couple of simulations to validate the proposed algorithms and analyze the performance. The real satellite and UAV connections are built from the Satellite Tool Kit (STK), and then put into MATLAB for further processing by the designed algorithms. Optimization tools CVX and GUROBI are also employed.

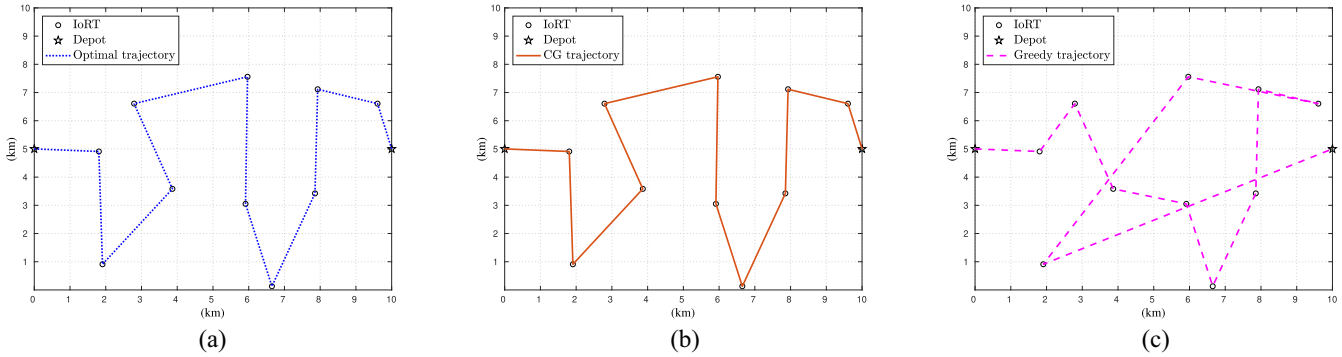

Fig. 5. UAV trajectory by different algorithms ($|\mathcal{I}| = 10$, $|\mathcal{U}| = 1$). (a) UAV optimal trajectory. (b) UAV trajectory from column generation. (c) UAV greedy trajectory.

A. Simulation Setup

Simulation parameters are listed in Table II. The Iridium-like LEO satellite networks are in the space segment, and there are 66 satellites distributed in 6 polar orbits, i.e., 11 satellites in each orbit. The orbit height is 780 km with a period of 6028 s. Moreover, these satellites are distributed in the Walker constellation, and such LEO satellite networks guarantee global coverage and each UAV can connect with at least one satellite at any time. The IoRT sensors are randomly distributed in the area within a geographical size 10 km$\times$10 km. The IoRT data are randomly generated from 10 to 100 Mbits and each β_i is randomly chosen from $\{0, 1\}$ with a uniform distribution. The fixed-wing UAVs fly at an altitude of 1 km in the trajectory stage [42]. The reference SNR at $l_{iu}(t) = 1$ m is $\gamma_0 = 80$ dB [29]. The speed of UAV in the intermediate trajectory segment is $v_u = 50$ m/s. The values of κ_1 and κ_2 are 9.26×10^{-4} kg/m and 2250 kg $\cdot$ m$^3/s^4$, respectively [43]. The power efficiency of UAV is $\theta = 70\%$ [44]. Since the data from an IoRT sensor is transmitted to a UAV when the UAV passes and the UAV flies at a very high altitude, we assume the distance between the IoRT sensor and UAV is the vertical distance, i.e., $l_{iu}(t) = 1$ km. The transmission power of IoRT sensor is P_{it}^{tr} =0.5 W, and the bandwidth from the IoRT sensor to the UAV is $B_{iu}^{t} = 2$ MHz. Following [32], the UAV transmission power is set as P_{ut}^{tr}=10 W, and the antenna gain is $G_u^{tr}G_s^{re} = 15$ dB, the carrier frequency is $f = 2.4$ GHz, and the bandwidth from UAVs to satellites is $B_{us}^{t} = 54$ MHz. The Boltzmann's constant is $k_B = 1.38\times10^{-23}$ J/K and the system noise temperature is 1000K.

B. Performance Analysis

To effectively evaluate the proposed column generation (CG) algorithm, in Fig. 4, the optimal solution of P0 is obtained by the branch-and-bound algorithm and serves as an optimal benchmark, i.e., the lower bound to measure the designed algorithms, and the greedy method based on choosing the nearest IoRT node for UAV trajectory is also set as a comparison. In detail, two UAVs participate, and the number of IoRT nodes ($|\mathcal{I}|$) changes from 20 to 200. From Fig. 4(a), compared with exponential complexity of the optimal solution, CG has a lower time complexity especially when the number of IoRT nodes is large. Meanwhile, Fig. 4(b) shows

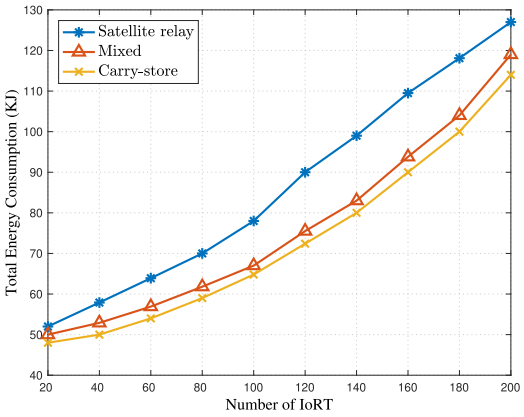

Fig. 6. Total energy cost in different transmission modes, $|\mathcal{U}| = 1$.

the total energy consumption results from different solution mechanisms, and the CG achieves the near-optimal solution, while the greedy method leads to a higher energy cost. Hence, the proposed CG is demonstrated to achieve the near-optimal solution with lower time complexity, which is applicable to the practical large-scale system.

To clearly show the UAV end-to-end trajectory solved from different algorithms, we consider ten randomly distributed IoRT sensors ($|\mathcal{I}| = 10$) and one UAV $|\mathcal{U}| = 1$) in the area, as shown in Fig. 5. Fig. 5(a) is the optimal trajectory solved by branch-and-bound, and Fig. 5(b) is the trajectory solved by the proposed column generation. We can observe that using the column generation obtains the same trajectory with the optimal solution. Besides, as a comparison, Fig. 5(c) shows the trajectory obtained by the greedy method, in which the nearest IoRT node is set as the next visiting node in the UAV trajectory. The total trajectory path is with long distances, and it also accounts for the high energy cost of the greedy algorithm in Fig. 4(b).

We also study the impacts of different data transmission modes to the system in Fig. 6. Three transmission modes are shown in Fig. 6: 1) the pure satellite relay mode; 2) the pure carry-store mode of UAV; and 3) the mixed transmission mode. In particular, different transmission modes cannot be completed by the same UAV. As expected, compared with the satellite relay mode, both the carry-store mode and the mixed mode consume fewer energy, and the reason lies in

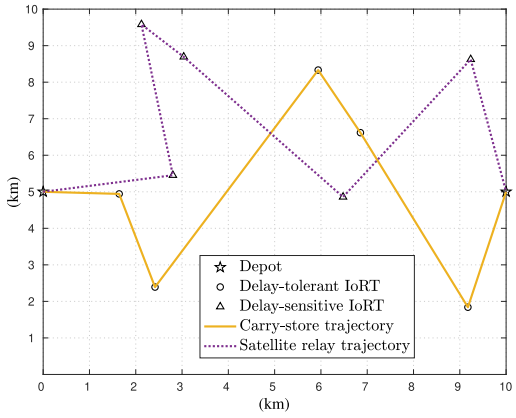

(a)

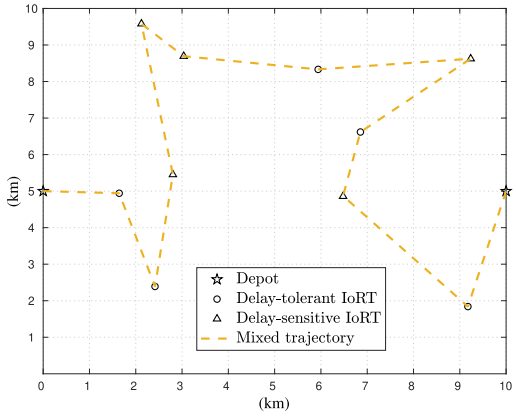

(b)

Fig. 7. UAV trajectory in different transmission modes ($|\mathcal{I}| = 10$). (a) UAV trajectory for separate delay-sensitive and delay-tolerant IoRT ($|\mathcal{U}| = 2$). (b) UAV trajectory for mixed delay-sensitive and delay-tolerant IoRT ($|\mathcal{U}| = 1$).

that the data transmission from UAVs to satellites also consumes energy. In the mixed mode, two types IoRT data can be transmitted by one UAV, which further reduce the total cost.

Moreover, the specific UAV trajectory paths in different modes are clearly depicted in Fig. 7. Ten IoRT sensors are decomposed into two parts according to whether the IoRT data is delay-tolerant or delay-sensitive. In Fig. 7(a), two UAVs are applied for the different data transmission modes: the satellite relay mode for the delay-sensitive IoRT data and the UAV carry-store mode for the delay-tolerant mode. Each mode is independently solved by column generation. In comparison to the mixed data relay trajectory by one UAV in Fig. 7(b), the separate mode not only needs more UAVs, which increases the capital expenditure and operation expenditure for UAVs, and the separate trajectory result in more energy cost, in accordance with the results in Fig. 6.

VI. Conclusion

In this article, we have focused on the LEO satellite network-assisted UAV trajectory for the IoRT data collection. Two data transmission modes including the satellite retransmission for the delay-sensitive IoRT data collected by the UAV and the carry-store mode of the UAV for the delay-tolerant IoRT data. Due to the limited energy of UAVs and multiple energy cost, we have formulated the problem to minimize the total energy cost of UAVs while guaranteeing all the IoRT data are collected. Since the problem is NP-hard to solve, the Dantzig–Wolfe decomposition has been used to decompose the problem to a master problem and a couple of pricing problems, and then we have designed the column generation-based algorithms to solve the decomposed problems efficiently. To further reduce the time complexity, we have designed a heuristic algorithm to deal with the pricing problem, which has no effect on the quality of final solutions. Finally, simulations are performed and the results have verified the efficiency of the column generation algorithm, which can enable low time complexity while the gap is less than 0.5% of the NP-hard optimal solution.

References

[1] W. Saad, M. Bennis, and M. Chen, "A vision of 6G wireless systems: Applications, trends, technologies, and open research problems," *IEEE Netw.*, vol. 34, no. 3, pp. 134–142, May/Jun. 2020.

[2] Z. Zhang *et al.*, "6G wireless networks: Vision, requirements, architecture, and key technologies," *IEEE Veh. Technol. Mag.*, vol. 14, no. 3, pp. 28–41, Sep. 2019.

[3] M. Sheng, D. Zhou, R. Liu, Y. Wang, and J. Li, "Resource mobility in space information networks: Opportunities, challenges, and approaches," *IEEE Netw.*, vol. 33, no. 1, pp. 128–135, Jan. 2019.

[4] *Starlink*. [Online]. Available: https://www.starlink.com/

[5] M. Mozaffari, W. Saad, M. Bennis, Y. Nam, and M. Debbah, "A tutorial on UAVs for wireless networks: Applications, challenges, and open problems," *IEEE Commun. Surveys Tuts.*, vol. 21, no. 3, pp. 2334–2360, 3rd Quart., 2019.

[6] Y. Zeng, Q. Wu, and R. Zhang, "Accessing from the sky: A tutorial on UAV communications for 5G and beyond," *Proc. IEEE*, vol. 107, no. 12, pp. 2327–2375, Dec. 2019.

[7] Y. Yang, Z. Zheng, K. Bian, L. Song, and Z. Han, "Real-time profiling of fine-grained air quality index distribution using UAV sensing," *IEEE Internet Things J.*, vol. 5, no. 1, pp. 186–198, Feb. 2018.

[8] Z. Han, A. L. Swindlehurst, and K. J. R. Liu, "Smart deployment/movement of unmanned air vehicle to improve connectivity in MANET," in *Proc. IEEE Wireless Commun. Netw. Conf. (WCNC)*, vol. 1. Las Vegas, NV, USA, Apr. 2006, pp. 252–257.

[9] H. Zhang, L. Song, Z. Han, and H. V. Poor, "Cooperation techniques for a cellular Internet of unmanned aerial vehicles," *IEEE Wireless Commun.*, vol. 26, no. 5, pp. 167–173, Oct. 2019.

[10] H. Zhang, L. Song, and Z. Han, *Unmanned Aerial Vehicle Applications Over Cellular Networks for 5G and Beyond*. Cham, Switzerland: Springer, 2020.

[11] D. Zhou, M. Sheng, X. Wang, C. Xu, R. Liu, and J. Li, "Mission aware contact plan design in resource-limited small satellite networks," *IEEE Trans. Commun.*, vol. 65, no. 6, pp. 2451–2466, Jun. 2017.

[12] D. Bertsimas and J. N. Tsitsiklis, *Introduction to Linear Optimization*. London, U.K.: Athena Sci., Feb. 1997.

[13] W. Saad, Z. Han, M. Debbah, and A. Hjorungnes, "A distributed merge and split algorithm for fair cooperation in wireless networks," in *Proc. ICC Workshops IEEE Int. Conf. Commun. Workshops*, Beijing, China, May 2008, pp. 311–315.

[14] J. Desrosiers and M. E. Lübbecke, *A Primer in Column Generation*. Boston, MA, USA: Springer, 2005.

[15] F. Vanderbeck, "On Dantzig–Wolfe decomposition in integer programming and ways to perform branching in a branch-and-price algorithm," *Oper. Res.*, vol. 48, no. 1, pp. 111–128, Feb. 2000.

[16] S. Zhang, H. Zhang, B. Di, and L. Song, "Cellular cooperative unmanned aerial vehicle networks with sense-and-send protocol," *IEEE Internet Things J.*, vol. 6, no. 2, pp. 1754–1767, Apr. 2019.

[17] Z. Wang, R. Liu, Q. Liu, J. S. Thompson, and M. Kadoch, "Energy-efficient data collection and device positioning in UAV-assisted IoT," *IEEE Internet Things J.*, vol. 7, no. 2, pp. 1122–1139, Feb. 2020.

[18] M. Mozaffari, W. Saad, M. Bennis, and M. Debbah, "Mobile unmanned aerial vehicles (UAVs) for energy-efficient Internet of Things communications," *IEEE Trans. Wireless Commun.*, vol. 16, no. 11, pp. 7574–7589, Nov. 2017.

[19] S. Zhang, J. Yang, H. Zhang, and L. Song, "Dual trajectory optimization for a cooperative Internet of UAVs," *IEEE Commun. Lett.*, vol. 23, no. 6, pp. 1093–1096, Jun. 2019.
[20] M. Chen, M. Mozaffari, W. Saad, C. Yin, M. Debbah, and C. S. Hong, "Caching in the sky: Proactive deployment of cache-enabled unmanned aerial vehicles for optimized quality-of-experience," *IEEE J. Sel. Areas Commun.*, vol. 35, no. 5, pp. 1046–1061, May 2017.
[21] M. Mozaffari, W. Saad, M. Bennis, and M. Debbah, "Unmanned aerial vehicle with underlaid device-to-device communications: Performance and tradeoffs," *IEEE Trans. Wireless Commun.*, vol. 15, no. 6, pp. 3949–3963, Jun. 2016.
[22] X. Cheng, Q. Yao, M. Wen, C.-X. Wang, L.-Y. Song, and B.-L. Jiao, "Wideband channel modeling and intercarrier interference cancellation for vehicle-to-vehicle communication systems," *IEEE J. Sel. Areas Commun.*, vol. 31, no. 9, pp. 434–448, Sep. 2013.
[23] M. Monwar, O. Semiari, and W. Saad, "Optimized path planning for inspection by unmanned aerial vehicles swarm with energy constraints," in *Proc. IEEE Global Commun. Conf. (GLOBECOM)*, Abu Dhabi, UAE, Dec. 2018, pp. 1–6.
[24] J. Wang, C. Jiang, Z. Wei, C. Pan, H. Zhang, and Y. Ren, "Joint UAV hovering altitude and power control for space-air-ground IoT networks," *IEEE Internet Things J.*, vol. 6, no. 2, pp. 1741–1753, Apr. 2019.
[25] P. K. Sharma and D. I. Kim, "Secure 3D mobile UAV relaying for hybrid satellite-terrestrial networks," *IEEE Trans. Wireless Commun.*, vol. 19, no. 4, pp. 2770–2784, Apr. 2020.
[26] X. Li, W. Feng, Y. Chen, C. Wang, and N. Ge, "Maritime coverage enhancement using UAVs coordinated with hybrid satellite-terrestrial networks," *IEEE Trans. Commun.*, vol. 68, no. 4, pp. 2355–2369, Apr. 2020.
[27] N. Cheng *et al.*, "Space/aerial-assisted computing offloading for IoT applications: A learning-based approach," *IEEE J. Sel. Areas Commun.*, vol. 37, no. 5, pp. 1117–1129, May 2019.
[28] S. Yan, L. Qi, and M. Peng, "User access mode selection in satellite-aerial based emergency communication networks," in *Proc. IEEE Int. Conf. Commun. Workshops (ICC Workshops)*, Kansas City, MO, USA, May 2018, pp. 1–6.
[29] Y. Zeng, R. Zhang, and T. J. Lim, "Throughput maximization for UAV-enabled mobile relaying systems," *IEEE Trans. Commun.*, vol. 64, no. 12, pp. 4983–4996, Dec. 2016.
[30] M. Hua, Y. Wang, Z. Zhang, C. Li, Y. Huang, and L. Yang, "Power-efficient communication in UAV-aided wireless sensor networks," *IEEE Commun. Lett.*, vol. 22, no. 6, pp. 1264–1267, Jun. 2018.
[31] Y. Zeng and R. Zhang, "Energy-efficient UAV communication with trajectory optimization," *IEEE Trans. Wireless Commun.*, vol. 16, no. 6, pp. 3747–3760, Jun. 2017.
[32] D. D. Mrema and S. Shimamoto, "Performance of quadrifilar helix antenna on EAD channel model for UAV to LEO satellite link," in *Proc. Int. Conf. Collaboration Technol. Syst. (CTS)*, Denver, CO, USA, May 2012, pp. 170–175.
[33] S. Zhang, H. Zhang, B. Di, and L. Song, "Joint trajectory and power optimization for UAV sensing over cellular networks," *IEEE Commun. Lett.*, vol. 22, no. 11, pp. 2382–2385, Nov. 2018.
[34] T. M. Cabreira, C. D. Franco, P. R. Ferreira, and G. C. Buttazzo, "Energy-aware spiral coverage path planning for UAV photogrammetric applications," *IEEE Robot. Autom. Lett.*, vol. 3, no. 4, pp. 3662–3668, Oct. 2018.
[35] G. Nemhauser and L. Wolsey, *Computational Complexity*. New York, NY, USA: Wiley, 2014, pp. 114–145, ch. I-5.
[36] A. J. Conejo, E. Castillo, R. Manguez, and R. García-Bertrand, *Decomposition Techniques in Mathematical Programming: Engineering and Science Applications*. New York, NY, USA: Springer, 2006.
[37] F. Vanderbeck and M. Savelsbergh, "A generic view of Dantzig–Wolfe decomposition in mixed integer programming," *Oper. Res. Lett.*, vol. 34, no. 3, pp. 296–306, May 2006.
[38] F. Vanderbeck and L. A. Wolsey, *Reformulation and Decomposition of Integer Programs*. Heidelberg, Germany: Springer, 2010, pp. 431–502.
[39] K. Mehlhorn and M. Ziegelmann, "Resource constrained shortest paths," in *Algorithms—ESA 2000*, M. S. Paterson, Ed. Heidelberg, Germany: Springer, 2000, pp. 326–337.
[40] J. Y. Yen, "Finding the K shortest loopless paths in a network," *Manag. Sci.*, vol. 17, no. 11, pp. 712–716, Jul. 1971.
[41] C. Barnhart, E. L. Johnson, G. L. Nemhauser, M. W. P. Savelsbergh, and P. H. Vance, "Branch-and-price: Column generation for solving huge integer programs," *Oper. Res.*, vol. 46, no. 3, pp. 316–329, May 1998.
[42] A. A. Khuwaja, Y. Chen, N. Zhao, M. Alouini, and P. Dobbins, "A survey of channel modeling for UAV communications," *IEEE Commun. Surveys Tuts.*, vol. 20, no. 4, pp. 2804–2821, 4th Quart., 2018.
[43] J. Lee, K. Park, Y. Ko, and M. Alouini, "A UAV-mounted free space optical communication: Trajectory optimization for flight time," *IEEE Trans. Wireless Commun.*, vol. 19, no. 3, pp. 1610–1621, Mar. 2020.
[44] J. K. Stolaroff, C. Samaras, E. R. O'Neill, A. Lubers, A. S. Mitchell, and D. Ceperley, "Energy use and life cycle greenhouse gas emissions of drones for commercial package delivery," *Nat. Commun.*, vol. 9, no. 1, pp. 409–421, Feb. 2018.

Ziye Jia received the B.E. degree in communications engineering and the M.S. degree in electronics and communications engineering from Xidian University, Xi'an, China, in 2012 and 2015, respectively, where she is currently pursuing the Ph.D. degree in communications and information systems.

She was a visiting Ph.D. student with the Department of Electrical and Computer Engineering, University of Houston, Houston, TX, USA, from 2018 to 2020. Her current research interests include resource allocation and network function virtualization in space–air–ground networks.

Min Sheng (Senior Member, IEEE) joined Xidian University, Xi'an, China, in 2000, where she is currently a Full Professor and the Director of the State Key Laboratory of Integrated Services Networks. She has published over 200 refereed papers in international leading journals and key conferences in the area of wireless communications and networking. Her current research interests include space–terrestrial integration networks, intelligent wireless networks, and mobile ad hoc networks.

Dr. Sheng received the China National Funds for Distinguished Young Scientists in 2018. She is the Vice Chair of IEEE Xi'an Section. She is an Editor of the IEEE COMMUNICATIONS LETTERS and IEEE TRANSACTIONS ON WIRELESS COMMUNICATIONS.

Jiandong Li (Senior Member, IEEE) received the B.E., M.S., and Ph.D. degrees in communications engineering from Xidian University, Xi'an, China, in 1982, 1985, and 1991, respectively.

He has been a Faculty Member with the School of Telecommunications Engineering, Xidian University, since 1985, where he is currently a Professor and the Vice Director of the Academic Committee of State Key Laboratory of Integrated Service Networks. He was a Visiting Professor with the Department of Electrical and Computer Engineering, Cornell University, Ithaca, NY, USA, from 2002 to 2003. His major research interests include wireless mobile communication, and cognitive and self-organizing networks.

Prof. Li was awarded as a Distinguished Young Researcher from NSFC and Changjiang Scholar from Ministry of Education, China, respectively. He served as the General Vice Chair for ChinaCom 2009 and the TPC Chair of IEEE ICCC 2013.

Dusit Niyato (Fellow, IEEE) received the B.Eng. degree from the King Mongkut's Institute of Technology Ladkrabang, Bangkok, Thailand, in 1999, and the Ph.D. degree in electrical and computer engineering from the University of Manitoba, Winnipeg, MB, Canada, in 2008.

He is currently a Professor with the School of Computer Science and Engineering, Nanyang Technological University, Singapore. His research interests are in the area of energy harvesting for wireless communication, Internet of Things, and sensor networks.

Zhu Han (Fellow, IEEE) received the B.S. degree in electronic engineering from Tsinghua University, Beijing, China, in 1997, and the M.S. and Ph.D. degrees in electrical and computer engineering from the University of Maryland, College Park, MD, USA, in 1999 and 2003, respectively.

From 2000 to 2002, he was a Research and Development Engineer of JDSU, Germantown, MD, USA. From 2003 to 2006, he was a Research Associate with the University of Maryland. From 2006 to 2008, he was an Assistant Professor with Boise State University, Boise, ID, USA. He is currently a John and Rebecca Moores Professor with the Electrical and Computer Engineering Department as well as with the Computer Science Department, University of Houston, Houston, TX, USA. His research interests include wireless resource allocation and management, wireless communications and networking, game theory, big data analysis, security, and smart grid.

Dr. Han received an NSF Career Award in 2010, the Fred W. Ellersick Prize of the IEEE Communication Society in 2011, the EURASIP Best Paper Award for the Journal on Advances in Signal Processing in 2015, the IEEE Leonard G. Abraham Prize in the field of Communications Systems (Best Paper Award in IEEE JSAC) in 2016, and several best paper awards in IEEE conferences. He is 1% Highly Cited Researcher since 2017 according to Web of Science. He is also the Winner of 2021 IEEE Kiyo Tomiyasu Award, for outstanding early to mid-career contributions to technologies holding the promise of innovative applications, with the following citation: "for contributions to game theory and distributed management of autonomous communication networks." He was an IEEE Communications Society Distinguished Lecturer from 2015 to 2018, an AAAS Fellow since 2019, and an ACM Distinguished Member since 2019.